INL/CON-23-76030-Revision-0

Concept Study of Robotic Camera-Based Foreign Object Detection for EV Wireless Charging

July 2024

Bo Zhang, Yizhuo Chen

INL/CON-23-76030-Revision-0

Concept Study of Robotic Camera-Based Foreign Object Detection for EV Wireless Charging

Bo Zhang, Yizhuo Chen

July 2024

Idaho National Laboratory
Idaho Falls, Idaho 83415

http://www.inl.gov

Prepared for the
U.S. Department of Energy
Under DOE Idaho Operations Office
Contract DE-AC07-05ID14517

Concept Study of Robotic Camera-based Foreign Object Detection for EV Wireless Charging

Bo Zhang[1], and Yizhuo Chen[2]

1. Department of Energy Storage and Advanced Transportation, Idaho National Laboratory, Idaho Falls, ID USA

2. Department of Computer Science, University of Illinois Urbana Champaign, IL USA

Corresponding: bo.zhang@inl.gov

***Abstract*— Wireless charging of an electric vehicle (EV) is an emerging charging technology promising convenient, autonomous, and highly efficient EV charging without requiring heavy gauge cables. However, due to the strong electromagnetic field created by this process that surrounds the wireless charger, the presence of foreign objects can detrimentally interact with it, thus affecting wireless power transfer (WPT) performance or leading to harmful and unwanted safety risks. This paper presents the results for a concept study on a robotic camera-based foreign object detection (FOD) system, as a supplement to the industry-existing overlapped FOD coil array method, for EV wireless charging. A Raspberry PI 4 control board and compatible Raspberry PI Camera Module 2 are used to implement camera-based object detection. The FOD program was developed using a state-of-the-art deep learning object detection model with the OpenCV and Pytorch library and is compatible with camera module hardware. A dry-run test with Raspberry PI and a camera module was conducted and the preliminary FOD function was verified. The feasibility assessment is also validated by comparing the performance of five existing state-of-the-art deep learning object detection models for vehicles, animals, persons, and metals subsets, respectively. Satisfactory performance on the benchmark datasets is observed by the tests, but further improvements are needed in future work when detecting small-sized metallic objects. A programable robotic car is also under development as ongoing work for carrying the Raspberry PI and camera module while moving for the maintenance process.**

Keywords*— *wireless power transfer (WPT), wireless charging, electric vehicle (EV), foreign object detection (FOD)

I. Introduction

Compared with conductive charging systems, wireless power transfer (WPT) or inductive power transfer (IPT) systems promise convenient, autonomous, and highly efficient EV charging [1-4] without requiring heavy gauge cables that might lead to potential electrical and ergonomic hazards. The Society of Automotive Engineers (SAE) J2954 standard [5], "Wireless Power Transfer for Light-Duty Plug-in/Electric Vehicles and Alignment Methodology," defines typical power electronics circuit topologies and recommended coupler designs for WPT with power levels up to 22 kVA from the input/grid side. However, a side topic involving foreign object detection (FOD) has not been heavily studied and there are still existing engineering practice gaps.

The presence of foreign objects, especially those consisting of metals or having specific electromagnetic characteristics, can detrimentally interact with the WPT electromagnetic field around the wireless charging system and vehicle architecture. This interaction can impact WPT performance or lead to harmful and unwanted safety risks. Conventional FOD methods involve detecting the differences of voltage, current, power, power factor, quality factor, etc., of the ground side resonant circuit with and without foreign objects [1, 6]. But the very small differences with and without debris make it challenging to determine whether it is due to a foreign object or just signal noises. References [7, 8] have successfully used an overlapped FOD coil array with two reverse direction loops to detect the variance of electromagnetic distortion due to the FOD. A similar measuring mechanism is also studied in Reference [9]. But the additional overlap coil is a downside, which adds to system complexity. References [10, 11] presented an FOD system without overlapping detecting coils, but the structure of the detecting coil is complicated. References [12, 13] achieved FOD by measuring the quality factor of the circuit, which avoids adding additional detecting coils, but it is mainly designed for closer distance wireless charging—not EV charging applications with a large ground clearance.

This paper discusses the FOD for wireless charging applications. To further explore the potential FOD methodology applicable for industrial maintenance practice, this paper seeks to leverage computer vision methodology by using a robotic camera and associated Raspberry PI control printed circuit board (PCB), as a supplement to the overlapped FOD coil method, to achieve a practically feasible FOD system for maintenance. The

Bo Zhang and Yizhuo Chen contributed equally to this paper. This manuscript was authored by scientists at Idaho National Laboratory, operated by Battelle Energy Alliance with the U.S. Department of Energy under DOE Contract No. DE-AC07-05ID14517.

preliminary concept design, Raspberry PI PCB, camera module setup, and a dry-run to verify the detection function, as well as the algorithm feasibility evaluation, are presented.

II. Wireless Charging and Foreign Object Detection

The WPT consists of a 60 Hz grid voltage input, active front end converters/power electronics, a ground side high-frequency resonant circuit, a coil and shielding system, a vehicle-side coil, a shielding and resonant circuit, and the battery itself. Fig. 1(a) shows a typical WPT charging application scenario, while Fig. 1(b) provides a look at the associated circuit [4, 14, 15].

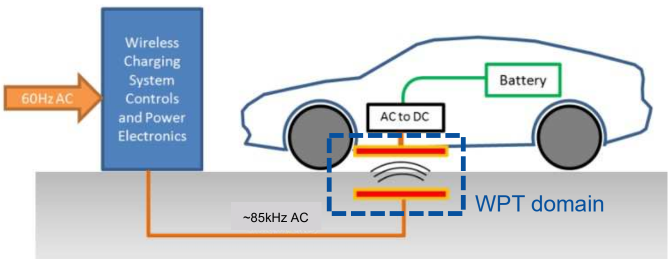

(a)

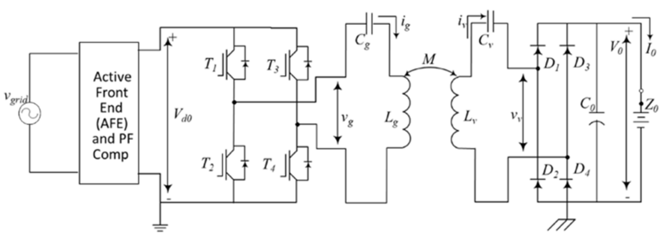

(b)

Fig. 1. (a) WPT application scenario. (b) The circuit schematic.

The electromagnetic coupling factor between the vehicle and charging pad is a key parameter determining WPT charging effectiveness. Assuming that the resistances of the coils are negligible compared to the inductances or load battery impedance of the coils, the output power, P_0, of WPT can be written as [16]:

$$P_0 = V_0 I_0 = v_v i_v = \omega M I_g I_v sin\varphi_{gv} \qquad (1)$$

where v_v and i_v present the transient vehicle-side voltage and current, respectively; I_g and I_v are the root mean square (RMS) values of the ground- and vehicle-side currents, respectively; M is the mutual inductance between the ground- and vehicle-side coils; and $sin\varphi_{gv}$ is the power factor on the vehicle-side.

Referring to Eq. (1), when foreign objects—especially those consisting of metals or having impactful electromagnetic characteristics—position within the WPT domain, as shown in the Fig. 1(a), the WPT electromagnetic field in the domain will interact with the foreign object, thus affecting the coupling coefficient and mutual inductance, M, and negatively impacting WPT performance or leading to an unwanted electromagnetic emission pattern.

The patents described in References [7, 8] employ an FOD system with an overlapped detecting coil to identify potential foreign objects, as shown in Fig. 2. As a commercial FOD system, an overlapped coil structure including two coil loops is used, but with current flowing in the reverse direction to achieve FOD while also eliminating blind spots. Normally, there would be no voltage occurring in the coil loops unless a metallic foreign object was positioned within the detection region, which will distort the electromagnetic (EM) field distribution slightly and lead to a reacting voltage in the detecting loops.

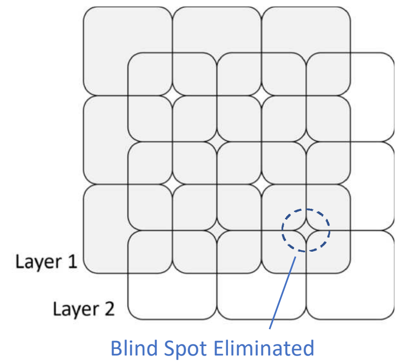

Fig. 2. FOD system with overlapped detecting coils [7, 8].

For the vast landscape of wireless charging parking lots or medium-duty/heavy-duty truck vocations, the overlapped detecting coil limits the detecting region and flexibility, while the positioning of the detecting coils between the ground side and the vehicle coils also adds to system complexity. The overlapped detecting coil array could be powered by the same or separate power supply, but this also adds an additional layer of complexity for maintenance.

III. Concept Design and Dry-Run

In addition to an overlapped detecting coil, a concept design FOD using a Raspberry PI PCB and camera is proposed to address the gap as a supplemental FOD method. The overlapped detecting coil can still be used to detect a metallic foreign object close to the charging pads, while the added camera detection system could provide additional detection scalability with a larger detection region, flexibility, and ease for routine maintenance. In the concept design, a Raspberry PI 4 PCB and compatible Raspberry PI Camera Module 2 are used to implement camera-based object detection. The FOD program is developed using deep learning object detection models with the OpenCV and Pytorch library in python coding language, which is compatible with the Raspberry PI Camera Module 2 hardware.

The "you only look once (YOLO)" detection system [17] is used as our model in this verification. Fig. 3 presents the early-stage FOD detection function verification showing preliminary detection is achieved, where foreign objects—including a mouse and a phone—could be detected as marked in red in Fig. 3. The number following "cell phone" or "mouse" indicates the probability of our detection (e.g., there is 69% chance this is a cell phone). The detection vision is displayed in a connected monitor/laptop via a high-definition multimedia interface (HDMI) cable; however, it should be noted that wireless video stream transfer to avoid a wired connection is further preferred and currently under development.

Fig. 3. Object detection dry-run with programmatic Raspberry PI and camera module.

A robotic vehicle is also proposed in the FOD system for carrying the Raspberry PI and camera module while moving along a designated maintenance route. Ideally, as shown in Fig. 4, the concept is to set up a pre-defined route in a parking lot. To avoid EM interference and shield a strong EM environment, a plastic robot car is currently adopted in the concept design, as demonstrated in Fig. 4. As the robot moves, its' turning is controlled wirelessly; associated ultrasonic seniors are employed as well for distance detection. Currently, the robotic car has functioned well in static camera operation or controlled running but without a camera media stream. Running fine-tuning when integrated with the Raspberry PI and camera module is still under development. Fig. 4 demonstrates the application scenario for a static wireless charging parking lot, while the concept also might be applicable to dynamic wireless charging.

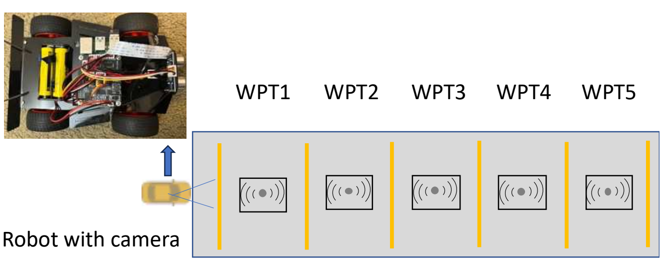

Fig. 4. Concept of robotic camera-based FOD for a wireless charging application in a parking lot.

IV. Feasibility Evaluation

To demonstrate the feasibility of using deep leaning models in our wireless charging FOD scenarios, we conducted preliminary experiments to evaluate the performance of five existing state-of-the-art deep learning object detection models, namely CO-DETR [18], ViTDet [19], DDQ [20], DINO [21], and RTMDet [22]. These models are constructed using neural networks and trained with a classical gradient descent. In the training phase, these models are fed with data points from various large-scale datasets, and then a loss is calculated with respect to the prediction and ground truth annotation for each batch of datapoints. The loss is then backpropagated to calculate the gradient from the loss to each parameter, while the parameters are adjusted with respect to the gradient. This process is iterated until the parameters converge. In the test phase, these models are evaluated on unseen test-set data points to verify their generalizability. These models have achieved strong performance on various benchmark computer vision datasets, which showed they may serve as strong candidates for our FOD tasks. Importantly, the trained parameters of these models are made available on the Internet for general use. Therefore, we can directly plug these models into our system to achieve immediate usability. Alternatively, we can also utilize these pretrained parameters as an initialization, and then fine-tune our own FOD models.

In the preliminary experiments, we used the MMDetection [23] implementation of these object detection models. MMDetection is an open-source detection method providing the fundamental tools and framework for developing an object detection program. It also reproduces the results of multiple state-of-the-art object detection models, and then provides the detailed configurations and pretrained parameters of these models so that users can readily understand and utilize them.

As for our evaluation benchmark dataset, we chose the MS COCO [24] 2017val dataset. The MS COCO dataset is a standard dataset used for training and evaluating object detection models. Its' 2017val version has been continuously used as a classical evaluation benchmark to compare different object detection models. The MS COCO dataset consists of 80 categories of objects from various domains—including vehicles, animals, appliances, people, etc. Each image in the MS COCO dataset contains multiple objects with their ground truth bounding box annotation and category annotations. A bounding box is a rectangle drawn to envelope an object, showing the location and size of that object. The task of object detection models is to predict the bounding box of each object seen in an image, and simultaneously predict the category of that object.

Following standard practices, we use the bounding box for Average Precision (AP) as our evaluation metric, which is a standard and comprehensive metric evaluating the performance of object detection algorithms. To understand bounding box AP, we first introduce Intersection over Union (IoU). For a specific pair of ground truth bounding box and predicted bounding box, IoU is defined as the area of the intersection of predicted bounding box and ground truth bounding box divided by the area of the union of the predicted bounding box and ground truth bounding box. IoU is defined in the range of 0 to 1. A large IoU indicates the predicted bounding box fits well to the ground truth bounding box. Bounding box AP is generally calculated at a specific IoU threshold. All predicted bounding boxes with an

IoU higher than the threshold are considered true positive, while all predicted bounding boxes with an IoU lower than the threshold are considered false positive. Bounding box AP is hence defined as the precision of bounding box prediction. To enhance comprehensiveness, bounding box AP is generally averaged over certain categories. For example, previous works primarily used AP_{50} and AP_{75}, which stand for the AP calculated at an IoU threshold of 0.5 and 0.75, respectively. To further boost comprehensiveness, previous works also introduced the concept of $AP_{50\text{-}95}$, which is the AP calculated and then averaged at various IoU thresholds ranging from 0.5 to 0.95, at a step of 0.05. More variants of AP include AP_s, AP_m, and AP_l, which stand for $AP_{50\text{-}95}$ averaged over small-sized objects, $AP_{50\text{-}95}$ averaged over medium-sized objects, and $AP_{50\text{-}95}$ averaged over large-sized objects, respectively. These metrics are widely adopted in previous object detection research to evaluate different aspects of proposed models and are all adopted in our experiments. Tab. 1 through Tab. 5 provide the results of these experiments.

Tab. 1. Comparison of state-of-the-art models on MS COCO datatset.

Model	$AP_{50\text{-}95}$	AP_{50}	AP_{75}	AP_s	AP_m	AP_l
CO-DETR	0.641	0.814	0.705	0.499	0.676	0.784
ViTDet	0.516	0.721	0.566	0.353	0.556	0.663
DDQ	0.587	0.768	0.645	0.416	0.629	0.743
DINO	0.584	0.771	0.642	0.415	0.622	0.735
RTMDet	0.564	0.742	0.618	0.416	0.601	0.710

Tab. 2. Comparison of models on MS COCO person subset.

Model	$AP_{50\text{-}95}$	AP_{50}	AP_{75}	AP_s	AP_m	AP_l
CO-DETR	0.718	0.916	0.797	0.553	0.772	0.875
ViTDet	0.610	0.862	0.672	0.411	0.681	0.796
DDQ	0.668	0.891	0.738	0.476	0.731	0.846
DINO	0.668	0.896	0.734	0.489	0.718	0.838
RTMDet	0.671	0.888	0.739	0.496	0.735	0.840

Tab. 3. Comparison of models on MS COCO vehicles subset.

Model	$AP_{50\text{-}95}$	AP_{50}	AP_{75}	AP_s	AP_m	AP_l
CO-DETR	0.671	0.857	0.725	0.515	0.650	0.820
ViTDet	0.570	0.795	0.612	0.378	0.546	0.725
DDQ	0.621	0.814	0.669	0.430	0.596	0.784
DINO	0.615	0.818	0.659	0.419	0.581	0.777
RTMDet	0.615	0.807	0.661	0.439	0.582	0.773

Tab. 4. Comparison of models on MS COCO animals subset.

Model	$AP_{50\text{-}95}$	AP_{50}	AP_{75}	AP_s	AP_m	AP_l
CO-DETR	0.782	0.929	0.855	0.606	0.806	0.875
ViTDet	0.684	0.883	0.755	0.482	0.718	0.791
DDQ	0.757	0.917	0.827	0.573	0.780	0.856
DINO	0.754	0.920	0.832	0.576	0.778	0.855
RTMDet	0.736	0.905	0.803	0.594	0.762	0.836

Tab. 5. Comparison of models on MS COCO metal subset.

Model	$AP_{50\text{-}95}$	AP_{50}	AP_{75}	AP_s	AP_m	AP_l
CO-DETR	0.617	0.797	0.676	0.548	0.701	0.786
ViTDet	0.421	0.596	0.461	0.301	0.541	0.625
DDQ	0.521	0.700	0.583	0.393	0.656	0.749
DINO	0.534	0.717	0.585	0.433	0.646	0.747
RTMDet	0.480	0.653	0.523	0.384	0.585	0.681

Tab. 1 summarized the performance of these models on the entire benchmark MS COCO 2017val dataset. It can be observed that all five models achieved high-performance on the MS COCO 2017val datasets. To be more specific, it is observed that all models achieved a higher than 0.721 AP_{50}, which means that if we take any predicted bounding boxes with an IoU higher than 0.5 with the ground truth bounding box as a true positive—meaning that all bounding boxes that are fitted half into the ground truth bounding boxes are viewed as correctly predicted—then all the models can achieve an averaged precision that is higher than 0.721 (e.g., out of 1000 predicted bounding boxes, at least 721 of them are correctly predicted). Similarly, it is observed that all the models achieved a higher than 0.566 AP_{75}, which means that if we take any predicted bounding boxes with an IoU higher than 0.75 with the ground truth bounding box as a true positive, then all the models can achieve an averaged precision higher than 0.566. We can also observe that all the models achieved a lower AP_{75} as compared to AP_{50}, which is expected because AP_{75} is calculated with a stricter IoU threshold (0.75) compared to AP_{50} (0.5). The predicted bounding boxes that are considered as correct for AP_{50} may not be considered as correct for P_{75}. Similarly, $AP_{50\text{-}95}$ tends to be even smaller as compared to AP_{75}, because the precision calculated at very high IoU thresholds are generally small, which lower the $AP_{50\text{-}95}$ down.

As for the AP_s, AP_m, and AP_l, the AP_s is observed to be smaller than the $AP_{50\text{-}95}$, while the AP_m and AP_l tend to be larger than the $AP_{50\text{-}95}$, which show these models are better at detecting medium-sized or large-sized objects than small-sized objects. This is partially due to the inherent difficulties in extracting representative features of a small object surrounded in a large and feature-rich context. Another possible reason is that it is difficult for the model to achieve high IoU for bounding boxes predicted for small objects, because a small shift of a bounding box may lead to a drastic change of IoU for small objects. As for the comparison between models, the CO-DETR model attained the highest scores for all metrics, showing its cutting-edge and comprehensive capability. It also is observed the models demonstrated consistency for all metrics. A model with high $AP_{50\text{-}95}$ tends to have high scores for other metrics as well.

To further examine the potential of deep learning models in FOD in our scenario, we selected four subsets from the MS COCO dataset—namely the person subset, vehicles subset, animals subset, and metal subset—and further evaluated five deep learning models on each of the subsets. The person, vehicles, and animals subsets are selected using the super-category provided by the MS COCO, while the metal subset was created by us, containing only spoon, fork, knife, and scissors categories. These four subsets are of more interest because the vehicles, animals, and person subsets consist of objects that can be commonly found in a wireless charging environment, and thus are considered as objects needing to be detected effectively so the EV can make proper reactions to them to avoid damaging accidents. Metal objects are also key objects needing to be detected since they may present the most detrimental influence on the charging process.

The evaluation results for the person, vehicles, animals, and metal subsets are presented in Tab. 2, Tab. 3, Tab. 4, and Tab. 5, respectively. It is observed from Tab. 2, Tab. 3, and Tab. 4 that all five models achieved higher performance on the person, vehicles, and animals subsets as compared to their overall performance on the entire MS COCO dataset. To be more specific, the $AP_{50\text{-}95}$ of the CO-DETR was 0.718, 0.671, and 0.782 for the person, vehicles, and animals subsets, respectively, which are all larger than 0.641 for the entire MS COCO dataset. Besides, it is observed that the AP_s, AP_m, and AP_l of CO-DETR for the person, vehicles, and animals subsets are mostly higher than that of CO-DETR for the entire MS COCO dataset, except for the AP_m on the vehicles subset. This observation reveals that CO-DETR's better performance for the person, vehicles, and animals subsets is not attributed to the size of the objects. Instead, it is because CO-DETR may extract finer features for these objects and can distinguish them from the context more effectively. These results showed the feasibility of applying state-of-the-art object detection models, especially CO-DETR in our FOD system, since they are particularly excelled in detecting objects of our interest.

Observing from Tab. 5, it is seen that all five models achieved a relatively lower performance on the metal subset as compared to their overall performance on the entire MS COCO dataset. However, it is observed that for CO-DETR, the AP_s, AP_m, and AP_l are still comparable with the entire MS COCO dataset. This result shows that although CO-DETR is not particularly adept at detecting metal objects, it is mainly due to the generally smaller size of metallic objects in the MS COCO dataset. This result points out the direction for future improvement, including improving the performance on detecting smaller metallic objects by fine-tuning the model on specially tailored FOD datasets, which can be constructed with multiple representative small metallic objects commonly found in a wireless charging environment. Another possible improvement is to equip our FOD system with multiple scale cameras and instruct the robot to capture fine-grained images when necessary. Besides, we also can observe that CO-DETR achieved the best performance for all subsets and metrics among the five evaluated models, which further substantiated its capability.

In summary, our preliminary evaluation validated that state-of-the-art object detection models are strong candidates for the proposed FOD system because of their strong performance on benchmark datasets, especially for vehicles, animals, and person subsets, which are of primary importance in our tasks. The preliminary evaluation also shows there is still room for improvement to adapt these models to our FOD environment, especially in detecting small-sized metallic objects.

V. Conclusion and Future Work

This paper presents a concept design for a robotic camera-based FOD system as a supplement to the industry-existing overlapped FOD coil array for an EV wireless charging maintenance application. A Raspberry PI 4 PCB and compatible Raspberry PI Camera Module 2 are used to achieve object detection. The FOD program is developed using a state-of-the-art deep learning object detection model with OpenCV and Pytorch library and is compatible with camera module hardware. A programable robotic car is also under development in the proposed FOD system for carrying the Raspberry PI and camera module while moving and operating for routine maintenance. The feasibility of applying state-of-the-art deep learning object detection models as a foreign object detector was also validated.

The proposed FOD system is still under development. A dry-run test with a programable Raspberry PI camera was demonstrated, but further integration with the robotic car is ongoing. The preliminary assessment validated the feasibility of the FOD algorithm, especially for vehicles, animals, person, and metals subsets. Future work is expected to focus on improving the performance of detecting smaller metallic objects by fine-tuning the model on specially tailored FOD datasets, which can be constructed with multiple representative small metallic objects commonly found in wireless charging environments. Another possible improvement is to equip our FOD system with multiple scale cameras and instruct the robot to capture fine-grained images when necessary. The impact of robot interference with a strong EM field environment also needs further investigation. Additional shielding measures might also be equipped if needed.

Acknowledgment

This work was supported by the DOE Vehicle Technologies Office. The authors thank E. J. Dufek, D. E. Smith, and T. D. Pennington from Idaho National Laboratory for management and lab coordination. The authors also thank L. Slezak from DOE for his project oversight and technical leadership.

REFERENCES

[1] D. Patil, M. Mcdonough, J. Miller, B. Fahimi, and P. Balsara, "Wireless Power Transfer for Vehicular Applications: Overview and Challenges,", *IEEE Transactions on Transportation Electrification,* Article vol. 4, no. 1, pp. 3-37, MAR 2018 2018, doi: 10.1109/TTE.2017.2780627.

[2] Z. Zhang, H. Pang, A. Georgiadis, and C. Cecati, "Wireless Power Transfer-An Overview,", *IEEE Transactions on Industrial Electronics,* Article vol. 66, no. 2, pp. 1044-1058, FEB 2019 2019, doi: 10.1109/TIE.2018.2835378.

[3] G. Covic and J. Boys, "Inductive Power Transfer,", *Proceedings of the Ieee,* Article vol. 101, no. 6, pp. 1276-1289, JUN 2013 2013, doi: 10.1109/JPROC.2013.2244536.

[4] B. Zhang *et al.*, "Quasi-Dynamic Electromagnetic Field Safety Analysis and Mitigation for High-Power Dynamic Wireless Charging of Electric Vehicles," in *2021 IEEE Transportation Electrification Conference & Expo (ITEC)*, 21-25 June 2021 2021, pp. 1-7, doi: 10.1109/ITEC51675.2021.9490192.

[5] SAEJ2954. "Wireless Power Transfer for Light-Duty Plug-in/Electric Vehicles and Alignment Methodology." [online] available: https://www.sae.org/standards/content/j2954_202010/. (accessed Nov. 1, 2020).

[6] T. R. Chun and M. Chris, "Foreign Object Detection," in *Wireless Power Transfer for Electric Vehicles and Mobile Devices*: IEEE, 2017, p. 1.

[7] A. M. Roy *et al.*, "Foreign object detection in wireless energy transfer systems," ed: US Patents: US9465064B2, 2016.

[8] S. Verghese, M. P. Kesler, K. L. Hall, and H. T. Lou, "Foreign object detection in wireless energy transfer systems," ed: US Patents: US9442172B2, 2016.

[9] J. Lu, G. Zhu, and C. Mi, "Foreign Object Detection in Wireless Power Transfer Systems,", *IEEE Transactions on Industry Applications,* Article vol. 58, no. 1, pp. 1340-1354, JAN 2022 2022, doi: 10.1109/TIA.2021.3057603.

[10] S. Y. Jeong, H. G. Kwak, G. C. Jang, S. Y. Choi, and C. T. Rim, "Dual-Purpose Nonoverlapping Coil Sets as Metal Object and Vehicle Position Detections for Wireless Stationary EV Chargers," *IEEE Transactions on Power Electronics,* vol. 33, no. 9, pp. 7387-7397, 2018, doi: 10.1109/TPEL.2017.2765521.

[11] S. Y. Jeong, V. X. Thai, J. H. Park, and C. T. Rim, "Self-Inductance-Based Metal Object Detection With Mistuned Resonant Circuits and Nullifying Induced Voltage for Wireless EV Chargers," *IEEE Transactions on Power Electronics,* vol. 34, no. 1, pp. 748-758, 2019, doi: 10.1109/TPEL.2018.2813437.

[12] S. C. Terry, "Wireless power systems with foreign object detection," ed: Google Patents, 2022.

[13] A. L. Schwartz, N. R. Mehrabadi, and H. Sepahvand, "Wireless Power Systems With Foreign Object Detection," ed: Google Patents, 2021.

[14] V. P. Galigekere *et al.*, "Design and Implementation of an Optimized 100 kW Stationary Wireless Charging System for EV Battery Recharging," in *2018 IEEE Energy Conversion Congress and Exposition (ECCE)*, 23-27 Sept. 2018 2018, pp. 3587-3592, doi: 10.1109/ECCE.2018.8557590.

[15] B. Zhang, R. B. Carlson, V. P. Galigekere, O. C. Onar, and J. L. Pries, "Electromagnetic Shielding Design for 200 kW Stationary Wireless Charging of Light-Duty EV," in *2020 IEEE Energy Conversion Congress and Exposition (ECCE)*, 11-15 Oct. 2020 2020, pp. 5185-5192, doi: 10.1109/ECCE44975.2020.9235329.

[16] B. Zhang, R. B. Carlson, J. G. Smart, E. J. Dufek, and B. Liaw, "Challenges of Future High Power Wireless Power Transfer for Light-duty Electric Vehicles----Technology and Risk Management," *eTransportation,* vol. 2, p. 100012, 2019/11/01/ 2019, doi: https://doi.org/10.1016/j.etran.2019.100012.

[17] J. Redmon, S. Divvala, R. Girshick, and A. Farhadi, "You only look once: Unified, real-time object detection," 2016, pp. 779-788.

[18] Z. Zong, G. Song, and Y. Liu, "Detrs with collaborative hybrid assignments training," 2023, pp. 6748-6758.

[19] Y. Li, H. Mao, R. Girshick, and K. He, "Exploring plain vision transformer backbones for object detection," 2022: Springer, pp. 280-296.

[20] S. Zhang *et al.*, "Dense distinct query for end-to-end object detection," 2023, pp. 7329-7338.

[21] H. Zhang *et al.*, "Dino: Detr with improved denoising anchor boxes for end-to-end object detection," *arXiv preprint arXiv:2203.03605,* 2022.

[22] C. Lyu *et al.*, "Rtmdet: An empirical study of designing real-time object detectors," *arXiv preprint arXiv:2212.07784,* 2022.

[23] K. Chen *et al.*, "MMDetection: Open mmlab detection toolbox and benchmark," *arXiv preprint arXiv:1906.07155,* 2019.

[24] T.-Y. Lin *et al.*, "Microsoft coco: Common objects in context. Computer Vision-ECCV 2014: 13th European Conference, Zurich, Switzerland, September 6-12, 2014," *Proceedings, Part,* vol. 13.